Progress of Theoretical Physics, Vol. 81, No. 1, January 1989

# Scaling Structures and Statistical Mechanics of Type I Intermittent Chaos

Nobuyuki MORI, Tatsuharu KOBAYASHI, Hiroki HATA, Terumitsu MORITA, Takehiko HORITA and Hazime MORI

*Department of Physics, Kyushu University 33, Fukuoka 812*

(Received July 21, 1988)

Intermittent chaos exhibits regular laminar motions and irregular turbulent bursts alternately, indicating that its chaotic attractor has two different types of local structures. For type I intermittency just before the saddle-node bifurcation, it is shown that the two types of local structures can be captured by the fluctuation spectrum $h(\Lambda)$ of the coarse-grained local expansion rates $\Lambda$ of nearby orbits and their $q$-weighted average $\Lambda(q)$, $(-\infty<q<\infty)$. The spectrum $h(\Lambda)$ and the average $\Lambda(q)$ are obtained analytically for a piecewise linear Markov map which exhibits type I intermittency, and numerically for the logistic map just before the period-three window. Thus it turns out that $h(\Lambda)$ has a linear part between $\Lambda=\Lambda_1>0$ and $\Lambda=\Lambda_2=0$ with a slope $q_\delta$, leading to a discontinuous transition of $\Lambda(q)$ from $\Lambda_1$ to $\Lambda_2$ at $q=q_\delta$ as $q$ is increased across $q_\delta$. This represents a phase transition between the laminar motions and the turbulent bursts, and gives a new type of $q$-phase transition with $1.0>q_\delta>0.5$ in contrast to other three types of $q$-phase transitions with transition points $q_\alpha=2.0$, $q_\beta<0.5$ and $q_\gamma=1.0$. Thus statistical mechanics of chaotic attractors at the bifurcation points is fully developed for the nontrivial case.

## § 1. Introduction

Many efforts have been made in order to construct statistical mechanics of chaotic dynamical systems which is useful for exploring non-equilibrium open systems far from equilibrium.[1)~3)] Very recently, important physical quantities have been discovered; for example, the singularity spectrum $f(\alpha)$ of the natural invariant measure,[4)] and the fluctuation spectrum $h(\Lambda)$ of the coarse-grained local expansion rates $\Lambda$ of nearby orbits along the local unstable manifolds.[5)~7)] They are the coarse-grained quantities which correspond to the thermodynamic functions in statistical thermodynamics. These quantities are the scaling exponents which describe the *scaling structures* of chaotic attractors, and lead to the variational principles for the thermodynamic formalism of chaotic dynamical systems which relate various scaling structure functions to each other within each class.[2),4)~7)] The spectra $f(\alpha)$ and $h(\Lambda)$, however, belong to different classes so that their relation is beyond the thermodynamic formalism.[7)]

The next step is, therefore, to find a statistical-mechanical formalism of the scaling structures in terms of the orbital structures of chaotic attractors. Then it would be important to study a relevant bifurcation of chaos which brings about an eminent change of a chaotic attractor at the bifurcation point. The purpose of the present series of papers[8),9)] is, therefore, to characterize the chaotic attractors at the bifurcation points for various bifurcations by the scaling structures, and then elucidate the scaling structures from the orbital structures of the critical attractors.

In the present paper, we shall study a chaotic attractor just before the saddle-node bifurcation from the above viewpoint. Such a chaotic attractor is known to exhibit

type I intermittency and produce a time series which consists of regular laminar motions interrupted by irregular turbulent bursts intermittently.[1] The laminar motions between two successive bursts have different durations which are randomly distributed over the time series with a mean duration $\tau$. As the control parameter $a$ approaches the saddle-node bifurcation point $a_c$, the mean laminar time $\tau$ diverges like $\tau \propto |a-a_c|^{-\gamma}$ with a positive exponent $\gamma$.[1] Namely, as the bifurcation point is approached, a local structure which produces the laminar motions is created and grows up. Then a chaotic structure of the attractor is eroded so as to produce only shortlived turbulent bursts intermittently. Thus the chaotic attractor changes to have two different types of local structures which produce the laminar motions and the turbulent bursts, respectively. Then eminent critical phenomena occur. As will be shown later, the two types of local structures can be captured by the spectrum $h(\Lambda)$ from dynamical laws. This provides a basis for elucidating critical phenomena from the local orbital structures of the chaotic attractor.

The laminar motions in type I intermittency can be described by one-dimensional maps according to the bifurcation theory,[3] as shown by Pomeau et al. numerically and experimentally.[1),10] The orbital structures of the turbulent bursts depend on the system. The main features of their scaling structures, however, would not depend on details of the system. Therefore, we shall also represent the turbulent bursts by one-dimensional maps. As a universal map for the onset of chaos, we shall take the logistic map and study type I intermittency just before the period-three window.[11] Its power spectrum of orbits was investigated in the previous papers theoretically[12] and numerically.[13] Since it is difficult to study the map analytically, we shall also take a piecewise linear Markov map which was introduced by Shobu, Ose and Mori in order to obtain the power spectrum analytically.[14] This map is not the expanding map and referred to as the SOM map. This map will enable us to derive the scaling structure functions of type I intermittency analytically by deriving the largest eigenvalue of the Fujisaka-Inoue operator.[15] Thus it will be found that type I intermittency is governed by a striking statistical law. Namely, its spectrum $h(\Lambda)$ exhibits a remarkable linear part with a slope $1.0 > q_\delta > 0.5$, representing the extreme coherence of chaotic motions just before the saddle-node bifurcation. This leads to a new type of $q$-phase transition between the laminar motions and the turbulent bursts with a transition point $q_\delta$. It will be also shown numerically that the logistic map exhibits the same type of $q$-phase transition.

In § 2 we define the coarse-grained local expansion rates and summarize the dynamic scaling structure functions. In § 3 we introduce the Fujisaka-Inoue operator and develop its matrix representation for a piecewise linear Markov map. In § 4 we introduce the SOM map and derive its scaling structure functions and generalized entropies analytically. In § 5 we take the logistic map and numerically obtain its scaling structure functions, which exhibit the same type of $q$-phase transition as that of the SOM map. The last section is devoted to a summary and some remarks.

## § 2. Scaling structure functions

Let us consider a chaotic orbit $\{x_t\}$, $(t=0, 1, 2, \cdots)$ generated by a one-dimensional

map

$$x_{t+1}=f(x_t)\,, \tag{2·1}$$

where $f(x)$ maps an interval $I$ onto itself and is assumed to be ergodic in $I$. Then, for almost all initial points $x_0\in I$, the orbit $\{x_t\}$ takes a positive Liapunov exponent $\Lambda^\infty$. Following Fujisaka,[16] we define the coarse-grained local expansion rate

$$\Lambda_n(x_0)\equiv(1/n)\sum_{t=0}^{n-1}\ln|f'(x_t)| \tag{2·2}$$

for large $n$. Then, $\Lambda_n(x_0)$ converges to the unique value $\Lambda^\infty$ as $n$ increases. If $n$ is finite, however, $\Lambda_n(x_0)$ takes different values between a maximum value $\Lambda_{\max}$ and a minimum value $\Lambda_{\min}$, depending on the initial point $x_0$. The probability density for $\Lambda_n(x_0)$ to take a value around $\Lambda$ is given by

$$P(\Lambda;\,n)\equiv\langle\delta(\Lambda_n(x_0)-\Lambda)\rangle\,, \tag{2·3}$$

where $\langle\cdots\rangle$ denotes the ensemble average over the natural invariant measure with respect to $x_0$. For large $n$, $P(\Lambda;\,n)$ takes the scaling form[17]

$$P(\Lambda;\,n)=\exp\{-n\psi(\Lambda)\}P(\Lambda^\infty;\,n)\,, \tag{2·4}$$

where $\psi(\Lambda)\geqq 0$. The function $\psi(\Lambda)$ is a concave function which takes the minimum zero at $\Lambda=\Lambda^\infty$,[17] and gives the fluctuation spectrum of $\Lambda_n(x_0)$ around $\Lambda^\infty$.

To describe large fluctuations of $\Lambda_n(x_0)$ explicitly, we employ the thermodynamic formalism of dynamical systems[2),4)~7)] and introduce the dynamic partition function

$$Z_n(q)\equiv\int d\Lambda\; P(\Lambda;\,n)\exp[-n(q-1)\Lambda]\,,\qquad(-\infty<q<\infty) \tag{2·5}$$

and the temporal scaling exponent

$$\Phi_n(q)\equiv-(1/n)\ln Z_n(q)\,. \tag{2·6}$$

We further introduce the derivatives

$$\Lambda_n(q)\equiv d\Phi_n(q)/dq\,, \tag{2·7a}$$

$$=\int d\Lambda\; P(\Lambda;\,n)\Lambda\exp[-n(q-1)\Lambda]/Z_n(q)\,, \tag{2·7b}$$

$$\sigma_n(q)\equiv-d\Lambda_n(q)/dq\,, \tag{2·8a}$$

$$=n\int d\Lambda\; P(\Lambda;\,n)[\Lambda-\Lambda_n(q)]^2\exp[-n(q-1)\Lambda]/Z_n(q)\,, \tag{2·8b}$$

where $\sigma_n(q)\geqq 0$ and hence $\Lambda_n(q)$ is a non-increasing function of $q$. For $q=1$, $\Phi_n(1)=0$, $\Lambda_n(1)=\Lambda^\infty$ and $\sigma_n(1)$ gives the ordinary variance of fluctuations of $\Lambda$ around $\Lambda^\infty$. For large values of $|q|$, we have $\Phi_n(q)=\Lambda_{\max}q$ for $q\to-\infty$, $\Phi_n(q)=\Lambda_{\min}q$ for $q\to+\infty$, which leads to $\Lambda_n(-\infty)=\Lambda_{\max}$, $\Lambda_n(+\infty)=\Lambda_{\min}$. Thus the $q$-weighted averages with $q<1$ and $q>1$ can explicitly describe positive and negative large fluctuations of $\Lambda_n(x_0)$, respectively. $\psi(\Lambda)$ and $\Phi_n(q)$ are the temporal scaling exponents which describe the scaling structures of chaotic attractors. Hence these functions are called the scaling

structure functions.

In the limit $n\to\infty$, $\Phi_n(q)$ is related to Fujisaka's exponent $\lambda_q$ for the time series $u_t=\ln|f'(x_t)|$ by $\Phi_\infty(q)=(q-1)\lambda_{1-q}$.[16]

For large $n$, the integral (2·5) is dominated by the typical value $\Lambda(q)$ of $\Lambda$ which minimizes the potential

$$\phi_q(\Lambda)\equiv\psi(\Lambda)+(q-1)\Lambda \tag{2·9}$$

for given $q$. Hence, (2·6) reduces to [5)~7)]

$$\Phi_n(q)=\min_\Lambda \phi_q(\Lambda)=q\Lambda(q)-h(\Lambda(q))\,, \tag{2·10a}$$

$$\Lambda_n(q)=\Lambda(q) \tag{2·10b}$$

for $n\to\infty$, where $h(\Lambda)\equiv\Lambda-\psi(\Lambda)$ and $h'(\Lambda)=q$. Therefore, $h(\Lambda)$ can be defined from $\Phi_\infty(q)$ by the Legendre transformation.[5),7)] The two spectra $\psi(\Lambda)$ and $h(\Lambda)$ are thus equivalent to each other, and the both are often used.[5)~9)] As will be shown later, for piecewise linear Markov maps, $\Phi_\infty(q)$ is related to the generalized entropies $K(q)$ by $\Phi_\infty(q)=(q-1)K(q)$. In the following, we shall mainly use $\psi(\Lambda)$. The limit $n\to\infty$ is called the temporal coarse-graining limit which is abbreviated as the TCG limit.

## § 3. Largest eigenvalue $\nu(q)$ of the Fujisaka-Inoue operator $H_q$

Since $f(x)$ is ergodic in the interval $I$, there exists a natural invariant density $\rho(x)$ defined by

$$\rho(x)\equiv\lim_{N\to\infty}(1/N)\sum_{t=0}^{N-1}\delta(x-x_t)\,. \tag{3·1}$$

The ensemble average of a function $G(x)$ over the natural invariant measure can be written as

$$\langle G(x)\rangle=\int dx\ \rho(x)G(x) \tag{3·2}$$

so that (2·5) and (2·3) lead to

$$Z_n(q)=\int dy\ \rho(y)\exp[-n(q-1)\Lambda_n(y)]\,. \tag{3·3}$$

Recently Fujisaka and Inoue discovered the important linear operator $H_q$,[15]

$$H_qG(x)\equiv\int dy\ \delta(f(y)-x)\exp[-(q-1)\ln|f'(y)|]G(y)\,, \tag{3·4a}$$

$$=\textstyle\sum_j G(y_j)/|f'(y_j)|^q\,, \tag{3·4b}$$

where $\sum_j$ denotes the sum over $y_j$'s satisfying $f(y_j)=x$ in $I$. This reduces to the Frobenius-Perron operator for $q=1$. Inserting $1=\int dx\ \delta(f(y)-x)$ into (3·3) and using (3·4a), we get

$$Z_n(q)=\int dx\ H_q^n\rho(x)\,, \tag{3·5}$$

where $Z_n(1)=1$ is ensured by $H_1\rho(x)=\rho(x)$.

Let $\nu(q)$ be the eigenvalue of $H_q$ whose absolute value is the largest among relevant eigenvalues. Expanding $\rho(x)$ in terms of the eigenfunctions of $H_q$, we find that, for $n\to\infty$, (3·5) reduces to $Z_n(q)\sim|\nu(q)|^n$ so that (2·6) leads to the basic relation[15]

$$\Phi_\infty(q)=-\ln|\nu(q)|\,. \tag{3·6}$$

Then $\Lambda_\infty(q)$, $\sigma_\infty(q)$ and $\psi(\Lambda)$ can be obtained from (2·7a), (2·8a) and (2·10). Thus the scaling structure functions are simply connected to the largest eigenvalue $\nu(q)$ in the TCG limit $n\to\infty$. Then the problem reduces to how to get $\nu(q)$ explicitly. Unfortunately, in most cases, it is difficult to get $\nu(q)$ analytically. But there are a few exceptions. For example, if the map $f(x)$ is Markov and piecewise linear on the Markov partition, then it is possible in the following manner.

The map $f: I\to I$ is called Markov if $I$ is divided into $M$ subintervals by $(M+1)$ points $p_0<p_1<\cdots<p_M$ such that $f(p_i)\in\{p_0, p_1, \cdots, p_M\}$ for any $i$ and $f$ is monotonic in each subinterval $I_i\equiv(p_{i-1}, p_i)$. Then the partition $\{I_i\}_{i=1}^{M}$ is called a Markov partition. Such a partition is possible only when $\Lambda_{\min}\geqq 0$, since otherwise there exists a stable periodic orbit with a negative Liapunov exponent. Let $f(x)$ be a piecewise linear Markov map, where its slope $f'(x)$ takes a constant value $f_i'$ within the subinterval $I_i$. Then $\rho(x)$ is a step function on the Markov partition and, as will be shown in Appendix A, $H_q$ can be represented by the $M\times M$ matrix whose elements are

$$(H_q)_{ij}=\begin{cases}|f'_j|^{-q} & \text{if} \quad f(I_j)\supseteqq I_i\,,\\ 0 & \text{otherwise}\,,\end{cases} \tag{3·7}$$

where we are restricted to the functional space of step functions on the Markov partition. Then $\nu(q)$ can be obtained from this matrix analytically so that the scaling structure functions in the TCG limit can be derived from the map (2·1) analytically.

As the simplest model for the turbulent bursts in intermittent chaos, let us take the tent map $f(x)=a^{-1}x, (0\leqq x\leqq a), b^{-1}(1-x), (a\leqq x\leqq 1)$ with $a+b=1$. Then the matrix takes the form

$$H_q=\begin{pmatrix} a^q & b^q \\ a^q & b^q \end{pmatrix}\,, \qquad (1>a, b>0) \tag{3·8}$$

whose largest eigenvalue is $\nu(q)=a^q+b^q$. Hence (3·6), (2·7a) and (2·8a) lead to the following scaling structure functions:

$$\Phi_B(q)=-\ln(a^q+b^q)\,, \tag{3·9a}$$

$$\Lambda_B(q)=-(a^q\ln a+b^q\ln b)/(a^q+b^q)\,, \tag{3·9b}$$

$$\sigma_B(q)=a^qb^q(\ln a-\ln b)^2/(a^q+b^q)^2\,, \tag{3·9c}$$

where the suffix B has been added instead of $\infty$ since they give a model for the bursts. The generalized entropies $K(q)$ are given by

$$K(q)=\Phi_B(q)/(q-1)=[1/(1-q)]\ln(a^q+b^q)\,, \tag{3·10}$$

where $K(0)=\ln 2$, $K(1)=-a\ln a-b\ln b$. We have $\Lambda^\infty=\Lambda_B(1)=K(1)$, which takes the maximum value $\ln 2$ for $a=b=1/2$. If $a\geqq b$, then $\Lambda_{\max}=-\ln b$, $\Lambda_{\min}=-\ln a$.

## § 4. Type I intermittency in the SOM map

We now study intermittent chaos whose time series consists of regular laminar motions interrupted by irregular turbulent bursts intermittently. As the control parameter $a$ approaches a saddle-node bifurcation point $a_c$, type I intermittency arises and the chaotic attractor changes to exhibit two types of motions; the laminar motions and the turbulent bursts. Then the attractor must have two different types of local structures which produce the two types of motions. Such local structures can be captured by the scaling structure functions $\Phi_\infty(q)$ and $\psi(\Lambda)$ explicitly, as will be shown in the following.

Type I intermittency is commonly observed in various experiments.[1] As its model for which we can obtain the scaling structure functions analytically, we take the piecewise linear non-expanding map[14]

$$f(x)=\begin{cases} ax+0.2\,, & (0\leqq x\leqq c)\\ a^{-1}(x-0.8)+1\,, & (c\leqq x\leqq 0.8)\\ -b^{-1}(x-1)\,, & (0.8\leqq x\leqq 1)\end{cases} \tag{4·1}$$

where $1>a>a_c\equiv 0.6$, $b\equiv 0.2$ and $c\equiv 0.8/(1+a)$. Its graph with a laminar orbit for $a>a_c$ is shown in Fig. 1. The map is chaotic in the interval $I=[0,1]$ for $a>a_c$, but undergoes a saddle-node bifurcation at $a=a_c$ so that the map has a stable fixed point at $x=0.2/(1-a)$ for $a<a_c$. Since $a<1$, the map is not expanding. Its natural invariant density and power spectrum of orbits were obtained analytically in the previous paper.[14]

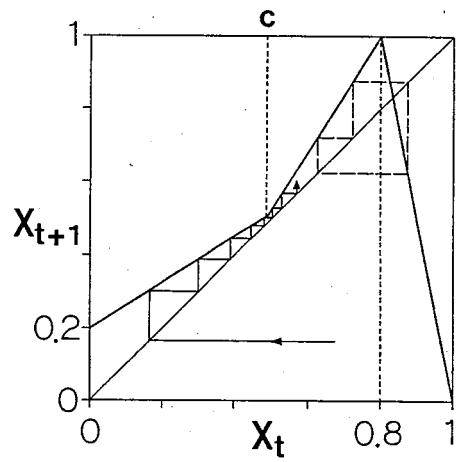


Fig. 1. Graph of the SOM map (4·1) with $a>a_c$, where a laminar orbit (thin solid line) and an unstable periodic orbit (dashed line) with period three are shown.

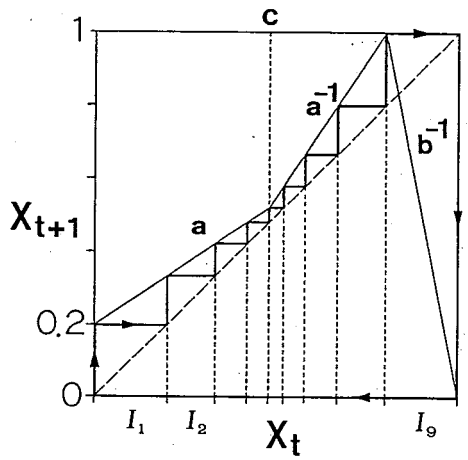


Fig. 2. Piecewise linear Markov map with $a=a_4\simeq 0.665$, $(m=4)$, where the period-ten orbit (heavy solid line) leads to the Markov partition $\{I_1, I_2, \cdots, I_9\}$.

Let us consider the chaotic attractor for $\varepsilon \equiv (a-a_c)/a_c \ll 1$, which has two types of local structures; a narrow channel around $x=c$ and an unstable period-three orbit around the fixed point $x=5/6$, as shown in Fig. 1. Any orbit $\{x_t\}$ with an initial point $x_0 < c$ spends much time for passing through the channel. Such an orbit undergoes a regular motion until $x_t$ goes beyond 0.8, producing a laminar motion. On the other hand, an orbit segment $\{x_t\}$ with $x_0 > 0.8$, which lies around the period-three orbit with a mean lifetime $\tau_B$, exhibits an irregular motion until $x_t$ goes beyond $1-bc$, representing a turbulent burst. When $x_t > 1-bc$, the orbit is reinjected into a laminar motion. The mean laminar time $\tau$ for passing through the channel becomes larger as $a$ approaches $a_c$. As shown in the previous paper,[14] the existence of such a large mean laminar time causes a singular power spectrum which consists of many spectral lines equally-spaced with separation $\Delta\omega = 2\pi/\tau$, their envelope obeying an inverse power law.

Let $a_m$ be the positive root of the algebraic equation[14]

$$a^{m+1} + a^m - 5a + 3 = 0\,, \qquad (m=3, 4, \cdots) \tag{4·2}$$

where $a_3 \simeq 0.743$, $a_m > a_{m+1}$, $a_\infty = a_c + 0$. This is the condition that $f^{2m}(0) = 0.8$ and $f^i(0) \leqq c$ for $i \leqq m$. Then the interval $I=[0, 1]$ is divided into $(2m+1)$ subintervals $\{I_i\}_{i=1}^{2m+1}$ with $I_i \equiv [f^{i-1}(0), f^i(0)]$, in each of which $f(x)$ is linear, as shown in Fig. 2 for $m=4$. Thus, at $a=a_m$, the map is Markov so that the matrix representation (3·7) can be used, leading to the $(2m+1)\times(2m+1)$ matrix

$$H_q = \left(\begin{array}{ccc|c} & & & b^q \\ \hline a_m^{-q} & & & b^q \\ & \ddots & & \vdots \\ & & a_m^{-q} & b^q \\ \hline & & a_m^{q} & b^q \\ & & & \vdots \\ & & & b^q \end{array}\right) \begin{array}{l} 1 \\ 2 \\ \\ m+1 \\ m+2 \\ \\ 2m+1 \end{array}, \tag{4·3}$$

where the unspecified elements are all zero. Its eigenvalue equation takes the form

$$\nu^{2m+1} - b^q\Big[\sum_{i=m}^{2m} a_m^{q(2m-i)}\nu^i + \sum_{i=0}^{m-1} a_m^{qi}\nu^i\Big] = 0\,. \tag{4·4}$$

The $\nu(q)$ of (3·6) is the largest real solution of this eigenvalue equation, which reduces to $\nu(q)=1$ for $q=1$, corresponding to $H_1\rho(x)=\rho(x)$. As shown in Appendix B, in the limit $m\to\infty$ with $a_\infty = a_c + 0$, we exactly obtain

$$\nu(q) = \begin{cases} 1 & \text{for} \quad q \geqq q_\delta \simeq 0.72716\,, \\ a_c^q + b^q & \text{for} \quad q \leqq q_\delta\,, \end{cases} \tag{4·5}$$

where $q_\delta$ is given by $[a_c^q + b^q]_{q=q_\delta} = 1$. Therefore, using (3·6), (2·7a) and (2·8a), we obtain

$$\Phi_\infty(q)=\begin{cases} 0 & \text{for} \quad q\geqq q_\delta\,, \\ -\ln(a_c{}^q+b^q) & \text{for} \quad q\leqq q_\delta\,, \end{cases} \tag{4·6}$$

$$\Lambda_\infty(q)=\begin{cases} 0 & \text{for} \quad q>q_\delta\,, \\ -(a_c{}^q\ln a_c+b^q\ln b)/(a_c{}^q+b^q) & \text{for} \quad q<q_\delta\,, \end{cases} \tag{4·7}$$

$$\sigma_\infty(q)=\begin{cases} 0 & \text{for} \quad q>q_\delta\,, \\ \infty & \text{for} \quad q=q_\delta\,, \\ a_c{}^q\, b^q(\ln a_c-\ln b)^2/(a_c{}^q+b^q)^2 & \text{for} \quad q<q_\delta\,, \end{cases} \tag{4·8}$$

where $a=a_c+0$, $\Lambda_{\max}=-\ln b\simeq 1.6094$, $\Lambda_{\min}=0$, $\Lambda^\infty=\Lambda_\infty(1)=0$. As will be shown in Appendix C, the generalized entropies are given by $K(q)=\Phi_\infty(q)/(q-1)$, so that (4·6) leads to

$$K(q)=\begin{cases} 0 & \text{for} \quad q\geqq q_\delta\,, \\ [1/(1-q)]\ln(a_c{}^q+b^q) & \text{for} \quad q\leqq q_\delta\,, \end{cases} \tag{4·9}$$

where $K(0)=\ln 2$, $K(1)=0$. Its derivative $K'(q)$ exhibits a discontinuous transition from $\Lambda_\infty(q_\delta-0)/(q_\delta-1)$ to zero at $q=q_\delta$. From (2·10a) we also obtain

$$\psi(\Lambda(q))=\begin{cases} 0 & \text{for} \quad q\geqq q_\delta\,, \\ (q-1)(a_c{}^q\ln a_c+b^q\ln b)/(a_c{}^q+b^q)-\ln(a_c{}^q+b^q) & \\ & \text{for} \quad q\leqq q_\delta\,. \end{cases} \tag{4·10}$$

Using (4·7) to eliminate $q$ from (4·10), we finally obtain

$$\psi(\Lambda)=\begin{cases} (1-q_\delta)\Lambda\,, & \text{for} \quad 0\leqq\Lambda\leqq\Delta\simeq 0.8517\,, \\ \Lambda+[g(\Lambda+\ln a_c)-g(\Lambda+\ln b)]/\ln(a_c/b)-\ln[\ln(a_c/b)] & \\ & \text{for} \quad \Delta\leqq\Lambda\leqq\Lambda_{\max}\,, \end{cases} \tag{4·11}$$

where $a=a_c+0$, $g(x)\equiv x\ln|x|$ and $\Delta\equiv\Lambda_\infty(q_\delta-0)$. The spectrum $h(\Lambda)=\Lambda-\psi(\Lambda)$ can be obtained from (4·11) easily. These functions are shown by the solid lines in Fig. 3.

Thus it turns out that, as $q$ is increased across $q_\delta$, the $q$-weighted average expansion rate $\Lambda_\infty(q)$ exhibits a discontinuous transition from $\Lambda_1=\Delta\equiv\Lambda_\infty(q_\delta-0)\simeq 0.8517$ to $\Lambda_2=0$ at $q=q_\delta$, at which $\sigma_\infty(q)$ diverges. This is a striking $q$-phase transition. Its physical meaning is the following. First, let us note that the scaling structure functions for $q<q_\delta$ have the same form as those for the tent map (3·9) and hence turns out to arise from the orbit segments $\{x_t\}$ lying within the interval $c<x_t<1-bc$ around the period-three orbit in Fig. 1. This means that the phase with $q<q_\delta$ represents the turbulent bursts which arise from the orbit segments $\{x_t\}$ with $x_0>0.8$ lying within the interval $c<x_t<1-bc$ with a mean lifetime $\tau_B$. The dashed lines in Fig. 3 show the extension of the branch of the turbulent bursts into the region $q>q_\delta$ or $\Lambda<\Delta$. Second, let us note that, for $a=a_m$, the laminar orbits $\{x_t\}$ with $x_0\in I_1$ lead to $\Lambda_n(x_0)=0$ for $n=2m$, since the contribution from $0<x_t<c$ is cancelled out by that from $c<x_t<0.8$, so that, for $n=\infty$, $\Lambda_{\min}=-\ln b/(2m+1)\to 0$ as $m\to\infty$. This means that the phase with $q>q_\delta$ represents the laminar motions which pass through the channel. Therefore, the $q$-phase transition of $\Lambda_\infty(q)$ from $\Lambda_1=\Delta$ to $\Lambda_2=0$ at $q=q_\delta$ is

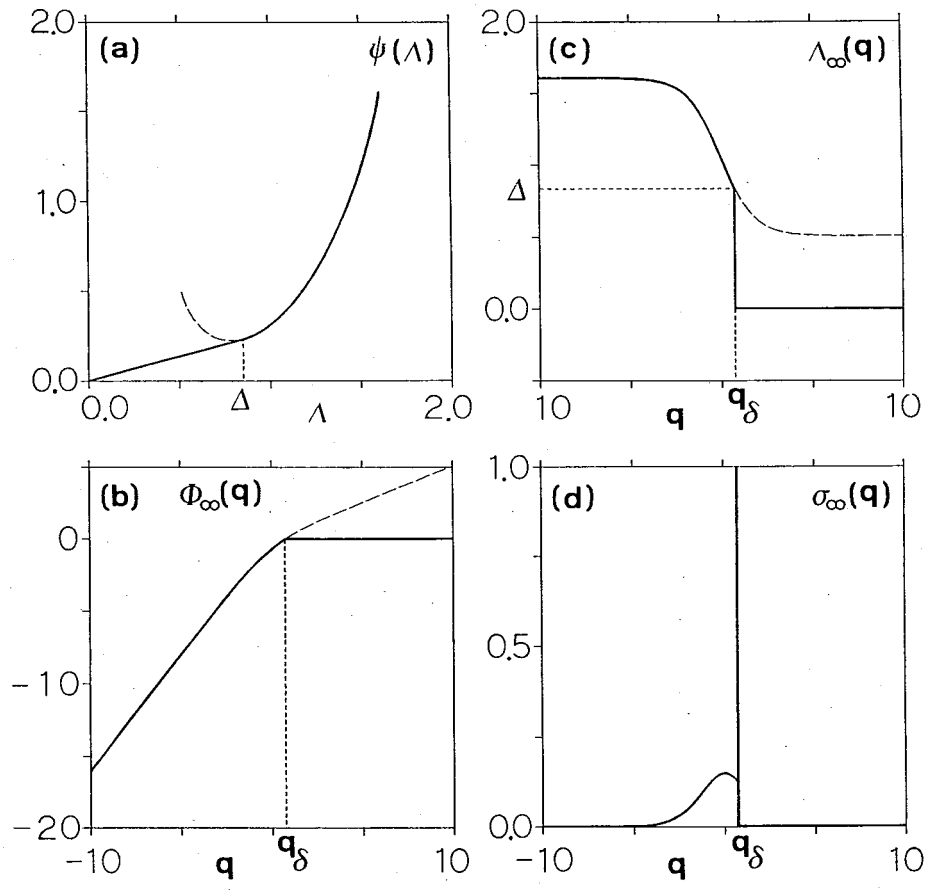


Fig. 3. Scaling structure functions of the SOM map with $a=a_c+0$. $\Lambda_\infty(q)$ exhibits a discontinuity $\Delta$ at $q=q_\delta$, at which $\sigma_\infty(q)$ diverges. $\psi(\Lambda)$ has a linear part with slope $s_\delta=1-q_\delta$ for $\Delta>\Lambda>0$. The dashed lines indicate the extension of the burst branch in the scaling structure functions.

the transition from the turbulent bursts to the laminar motions.

Here it should be noted that the limit $a\to a_c$ has been taken after the limit $n\to\infty$ has been taken with $a>a_c$ so that the orbits passing through the channel have been taken into account. Thus the $q$-phase transition characterizes the two dominant local structures of the chaotic attractor at $a=a_c+0$ in the clear-cut manner.

## § 5. Type I intermittency in the logistic map

The well-known logistic map is given by

$$x_{t+1}=f(x_t)=1-\mu x_t^2\,, \qquad (-1\leqq x_t\leqq 1) \tag{5·1}$$

which undergoes a period-three saddle-node bifurcation at $\mu=\mu_c=1.75$ and exhibits type I intermittency for $\mu<\mu_c$.[11),13)] The graph of $x_{t+3}$ vs $x_t$ for $\mu=1.74$ is shown in Fig. 4. Thus, as $\mu$ approaches $\mu_c$ from below, the chaotic attractor changes to have three narrow channels around $x=c_1, c_2, c_3$, which produce regular laminar motions

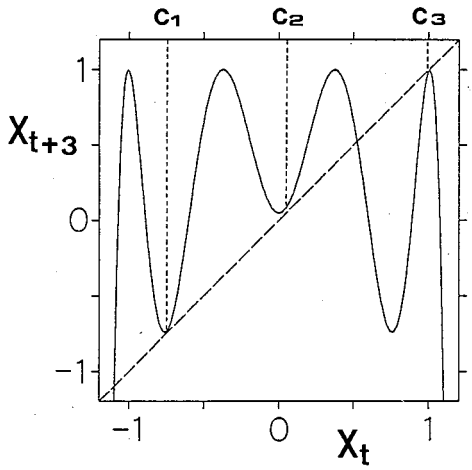


Fig. 4. Graph of the third iterate $f^3(x_t)$ of the logistic map (5·1) with $\mu=1.74<\mu_c$, which has three channels around $x=c_1, c_2, c_3$.

similar to that of Fig. 1. Then the chaotic attractor has two types of local structures; the narrow channels and an eroded chaotic structure which consists of steep line segments with $|df^3(x)/dx|>1$, as seen in Fig. 4. The eroded chaotic structure produces irregular turbulent bursts intermittently. In this case, however, it is difficult to get the largest eigenvalue $\nu(q)$ of $H_q$ analytically, since $\Lambda_{\min}<0$ so that a Markov partition does not exist. Since the logistic map is expected to give universal properties of type I intermittency, however, we have computed its scaling structure functions numerically. Its power spectrum of orbits was obtained numerically in the previous paper,[13] and turned out to have two eminent peaks at frequencies $\omega=0, 2\pi/3$ which consist of many equally-spaced lines with separation $\Delta\omega=2\pi/\tau$, their envelopes obeying inverse-power laws.

The ensemble average in (2·3) can be given by

$$\langle G(x_0)\rangle\simeq(1/N)\sum_{t=0}^{N-1}G(x_t) \tag{5·2}$$

with a large $N$. By taking $n=300$, $N=0.9\times10^6$, we have computed the probability density (2·3) and then obtained the fluctuation spectrum $\psi(\Lambda)$ from

$$\psi_n(\Lambda)\equiv-(1/n)\ln[P(\Lambda;\, n)/P(\Lambda^\infty;\, n)] \tag{5·3}$$

with $\Lambda^\infty=\langle\Lambda_n(x_0)\rangle$, and the scaling structure functions $\Phi_n(q)$, $\Lambda_n(q)$ and $\sigma_n(q)$ from (2·5), (2·7b) and (2·8b), respectively. The results are shown in Fig. 5, where $\varepsilon\equiv49$ $(\mu_c-\mu)=4.9\times10^{-3}$;

$$\tau=3\pi/\sqrt{\varepsilon}\simeq135\,, \tag{5·4a}$$

$$q_\delta\simeq0.925\,,\qquad \Lambda^\infty\simeq0.075\,. \tag{5·4b}$$

Thus it turns out that $\sigma_n(q)$ has a sharp peak at $q=q_\delta$, and the largest-term approximation (2·10b), shown by the crosses +'s, has a clear discontinuity from $\Lambda_1\simeq0.46$ to $\Lambda_2\simeq0.08$ at $q=q_\delta$. Since $n\gg\tau$, these indicate that, for $\mu=\mu_c-0$, $\Lambda_\infty(q)$ exhibits a $q$-phase transition from $\Lambda_1>0$ to $\Lambda_2=0$ at $q=q_\delta$, at which $\sigma_\infty(q)$ diverges. This is the same type of $q$-phase transition as that of the SOM map, and represents the phase transition from the turbulent bursts to the laminar motions. Such $q$-phase transitions due to type I intermittency will be called the $q_\delta$-phase transitions.

It should be noted that, if a very large $N$ is taken so that $\ln N\gtrsim n$, then there appears a $q$-phase transition at $q=q_\alpha=2.0$ due to the quadratic extremum of $f(x)$ at $x=0$, as studied in the previous papers.[8]

The spectrum $\psi_n(\Lambda)$ has a remarkable linear part between $\Lambda=\Lambda_1$ and $\Lambda=\Lambda_2$, as

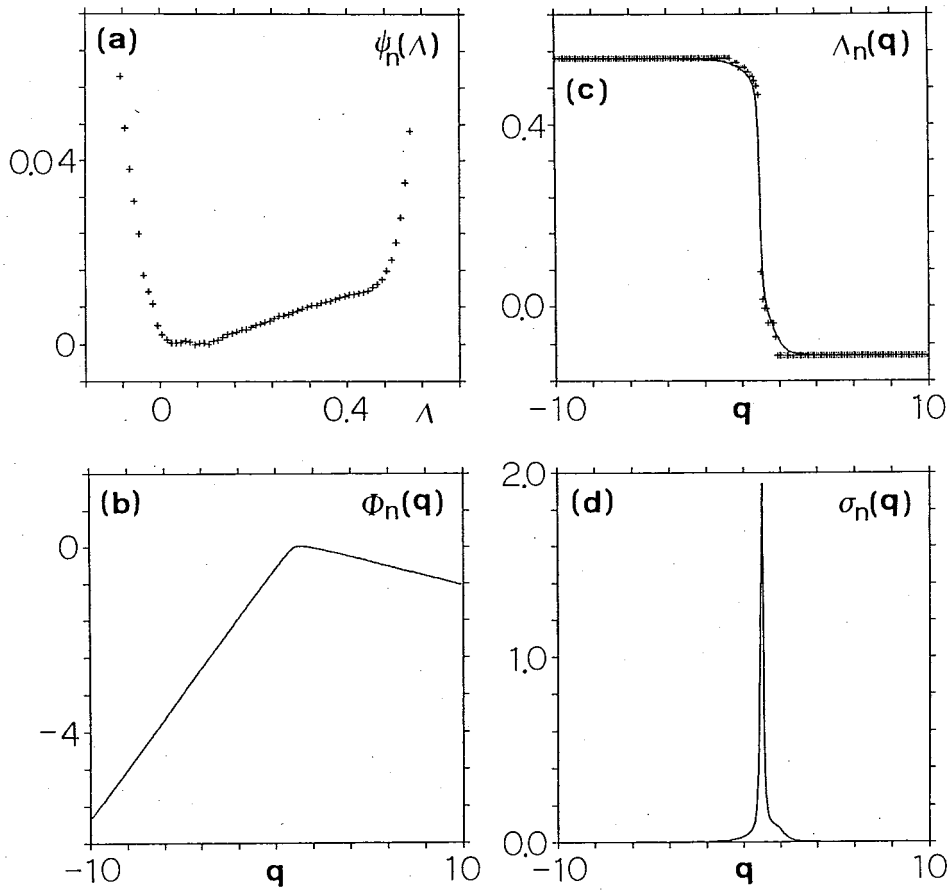


Fig. 5. Scaling structure functions of type I intermittency in the logistic map (5·1) just before the period-three window, where $\varepsilon\equiv 49(\mu_c-\mu)=4.9\times10^{-3}$, $n=300$, $N=0.9\times10^6$. $\Lambda_n(q)$ exhibits a discontinuity from $\Lambda_1\simeq 0.46$ to $\Lambda_2\simeq 0.08$ at $q=q_\delta\simeq 0.925$, at which $\sigma_n(q)$ has a sharp peak. $\psi(\Lambda)$ has a linear part with slope $s_\delta=1-q_\delta\simeq 0.075$ for $\Lambda_1>\Lambda>\Lambda_2$.

shown in Figs. 3 and 5. Its slope is given by

$$s_\delta\equiv 1-q_\delta=\begin{cases}0.273 & \text{for the SOM map}, \quad (5\cdot5a)\\ 0.075 & \text{for the logistic map}. \quad (5\cdot5b)\end{cases}$$

This linear law represents the extreme coherence of chaotic motions just before the saddle-node bifurcation in strong contrast to the quadratic Gaussian spectrum for random processes. This is the origin of the $q_\delta$-phase transition, as can be seen in the following manner. Let the linear law hold for $\Lambda_1\geqq\Lambda\geqq\Lambda_2$ with slope $s_\delta$. Then the potential (2·9) takes the form

$$\phi_q(\Lambda)=(q-q_\delta)\Lambda+C \quad (5\cdot6)$$

for $\Lambda_1\geqq\Lambda\geqq\Lambda_2$, where $C$ is a constant. Then the value $\Lambda(q)$ of $\Lambda$ which minimizes $\phi_q(\Lambda)$ is given by $\Lambda_1$ for $q<q_\delta$ and $\Lambda_2$ for $q>q_\delta$. Therefore, as $q$ is increased across $q_\delta$, $\Lambda_\infty(q)=\Lambda(q)$ exhibits a discontinuous transition from $\Lambda_1$ to $\Lambda_2$ at $q=q_\delta$ with a discontinuity $\Delta\equiv\Lambda_1-\Lambda_2$, at which the variance $\sigma_\infty(q)$ diverges. This is the $q_\delta$-phase

transition.

Since $h(\Lambda)=\Lambda-\psi(\Lambda)$, the linear part of $\psi(\Lambda)$ leads to the linear part of $h(\Lambda)$ between $\Lambda=\Lambda_1$ and $\Lambda=\Lambda_2$ with slope $h'(\Lambda)=q_\delta$. The spectrum $h(\Lambda)$ was first computed by Sano, Sato and Sawada[5] for the logistic map just before the period-three window. Since $h'(\Lambda)=q_\delta\simeq 0.925$, their result is not inconsistent with our result, although their computation was not precise enough to indicate the linear law of $h(\Lambda)$.

Since the logistic map has the quadratic extremum, we have $\psi(\Lambda_1)<\Lambda_1/2$ so that $s_\delta<1/2$.[9] Therefore, we may assume that the slope $s_\delta$ satisfies $0.5>s_\delta>0$ in contrast to other three types of $q$-phase transitions with slopes $s_\alpha=-1$, $s_\beta>0.5$ and $s_\gamma=0$.[8] This leads to the transition point $1.0>q_\delta>0.5$ in contrast to $q_\alpha=2.0$, $q_\beta<0.5$ and $q_\gamma=1.0$.

## § 6. A short summary and some remarks

A striking statistical law has been found to hold for type I intermittency. Namely, the fluctuation spectrum $\psi(\Lambda)$ of the coarse-grained local expansion rates $\Lambda$ has turned out to have a remarkable linear part between $\Lambda=\Lambda_1>0$ and $\Lambda=\Lambda_2=0$ with a slope $0.5>s_\delta>0$, as shown in Figs. 3 and 5. Since $h(\Lambda)=\Lambda-\psi(\Lambda)$, the linear part of $\psi(\Lambda)$ is equivalent to the linear part of $h(\Lambda)$ with a slope $h'(\Lambda)=q_\delta\equiv 1-s_\delta$. This linear law brings about a discontinuous transition of the $q$-weighted average $\Lambda_\infty(q)$ from $\Lambda_1$ to $\Lambda_2$ at $q=q_\delta$, as shown in Figs. 3 and 5.

This $q$-phase transition represents a phase transition between the regular laminar motions and the irregular turbulent bursts. The chaotic attractor of type I intermittency has two different types of local orbital structures. One is narrow channels around the region where a pair of unstable and stable periodic orbits are created by a saddle-node bifurcation, and the other is an eroded chaotic structure. These two types of local structures produce the laminar motions and the turbulent bursts, respectively. Consider a chaotic orbit. Then the phase with $q>q_\delta$ is governed by the orbit segments passing through the channels, whereas the phase with $q<q_\delta$ is dominated by the orbit segments lying in the eroded chaotic structure.

Thus the $q_\delta$-phase transition has been elucidated from the orbital structure of the chaotic attractor by taking two one-dimensional maps. One is the logistic map (5·1) which exhibits type I intermittency just before a period-three window. Although this is known as a universal map for the onset of chaos, its analytic study is difficult so that we have carried out a numerical study in § 5. The other is a piecewise linear Markov map (4·1) with the control parameter $a=a_m$, which can be studied analytically. Here it should be noted that, although the local expansion rate $f'(x)$ takes only three values $a$, $a^{-1}$, $-b^{-1}$, the coarse-grained local expansion rate $\Lambda_n(x_0)$ exhibits a great variety of behaviors and gives the characteristic features of type I intermittency. The situations are similar to a system of Ising spins whose magnetic moments take only two values but whose magnetization exhibits a great variety of phenomena, including a magnetic phase transition. $\psi(\Lambda)$, $K(q)$, $\Lambda_\infty(q)$ and other scaling structure functions for $a=a_m$ can be derived from the largest eigenvalue $\nu(q)$ of the matrix (4·3) with the aid of (3·6). Thus, taking the limit $m\to\infty$, we have exactly derived the dynamical expressions (4·6)~(4·11) for the scaling structure functions and $K(q)$ for $a=a_c+0$,

which exhibit the $q_\delta$-phase transition. The present theory thus gives one typical example for the statistical-mechanical formalism of the scaling structures.

For further developments, the following problems should be clarified.

(1) Critical phenomena around the bifurcation point $a_c$ with $\varepsilon \equiv |a-a_c|/a_c \ll 1$, in particular, critical anomalies of the scaling structure functions are interesting and important phenomena. We may expect the following temporal scaling laws for the deviations of $\psi_n(\Lambda)$ and $\Phi_n(q)$ from those at $\varepsilon=0$:

$$\Delta\psi_n(\Lambda)=\tau^{-\eta}B(\hat{\Lambda}\tau^{\xi}, n/\tau)\,, \tag{6·1}$$

$$\Delta\Phi_n(q)=\tau^{-\eta}C(\hat{q}\tau^{\eta-\xi}, n/\tau)\,, \tag{6·2}$$

where $\tau(\propto\varepsilon^{-\gamma})$ is the mean laminar time, $\hat{\Lambda}$ and $\hat{q}$ denote the differences of $\Lambda$ and $q$ from their some values, and $B(x, y)$ and $C(x, y)$ are functions of $x$ and $y$ which are independent of $\varepsilon$. The problem is whether there exist a limit $B(x, \infty)$ for $y\to\infty$ and a limit of the form

$$B(x, y)=y^{-\eta}b(xy^{\xi}) \qquad \text{for} \quad y\to 0 \tag{6·3}$$

or not, where the function $b(z)$ describes the critical region where $1\ll n\ll\tau$. For the SOM map, we have $\xi=0$, $\eta=1$.

(2) What scaling structures does the chaotic attractor of type III intermittency have? The laminar motions in type III intermittency can be described by an expanding one-dimensional map.[1),18),19)] Therefore, Szépfalusy et al.'s work[20)] suggests that type III intermittency brings about a transition of $\Lambda_\infty(q)$ and $K(q)$ since the second iterate of the map has slope unity at the fixed point. Then eminent critical phenomena also occur. Moreover we have similar problems for type II intermittency.

(3) How does type I intermittency give rise to a linear part for the singularity spectrum $f(\alpha)$ of the natural invariant measure in the two-dimensional maps? As shown in the previeus paper,[7)] $f(\alpha)$ is closely related to $h(\Lambda)\equiv\Lambda-\psi(\Lambda)$. Therefore, we may expect that $f(\alpha)$ has a linear part with slope $f'(\alpha)=q_D$ for $\alpha_1>\alpha>\alpha_2$, and the $q$-weighted average $\alpha(q)$ exhibits a discontinuous transition from $\alpha_1$ to $\alpha_2$ at $q=q_D$, where

$$q_D=q_\delta+\Phi_\infty(q_\delta)/|\ln|J||\,, \tag{6·4}$$

$J$ being the Jacobian of the map.[7)]

These problems will be studied in subsequent papers.

## Acknowledgements

We are extremely grateful to Dr. T. Yoshida, Professor H. Okamoto and all others of our group at Kyushu University for several useful and stimulating discussions. We also thank Professor H. Fujisaka and Professor M. Inoue for sending us their interesting papers and some useful discussions. This study was partially financed by the Grant-in-Aid for Scientific Research of Ministry of Education, Science and Culture.

## Appendix A

*—— Derivation of the Matrix (3·7) ——*

Since $\rho(x)$ is a step function, the relevant eigenfunctions of $H_q$ are also step functions. Therefore, we introduce the characteristic function for the subinterval $I_i$ of the Markov partition:

$$\chi_i(x)\equiv 1 \quad \text{if} \quad x\in I_i\,, \qquad 0 \quad \text{otherwise}\,. \tag{A·1}$$

Then any step function $F(x)$ can be written as $F(x)=\sum_{i=1}^{M}F_i\chi_i(x)$. Further we define the transition matrix $T_{ij}$ from $I_j$ to $I_i$:

$$T_{ij}\equiv 1 \quad \text{if} \quad f(I_j)\supseteqq I_i\,, \qquad 0 \quad \text{otherwise}\,. \tag{A·2}$$

Then (3·4b) leads to

$$H_q\chi_i(x)=\sum_j \chi_i(x)\,T_{ij}|f_j'|^{-q}\,, \tag{A·3}$$

$$H_qF(x)=\sum_i\sum_j F_i\chi_i(x)\,T_{ij}|f_j'|^{-q}=\sum_i G_i\chi_i(x)\,, \tag{A·4}$$

where $f_j'$ denotes the value of the slope $f'(x)$ in the subinterval $I_j$ and

$$G_i\equiv\sum_j F_i\,T_{ij}|f_j'|^{-q}\,. \tag{A·5}$$

Namely, the operator $H_q$ transforms a step function $F(x)$ to a step function $G(x)=\sum_i G_i\chi_i(x)$. Therefore $H_q$ can be represented by the $M\times M$ matrix

$$(H_q)_{ij}=T_{ij}|f_j'|^{-q} \tag{A·6}$$

as far as it operates on the step functions on the Markov partition. This leads to (3·7).

## Appendix B

*—— Derivation of (4·5) for $\nu(q)$ in the Limit $m\to\infty$ ——*

From (2·8b), we have $\sigma_\infty(q)\geqq 0$ for all $q$. Hence $\Lambda_\infty(q)$ is a non-increasing function with $\Lambda_\infty(-\infty)=\Lambda_{\max}$, $\Lambda_\infty(+\infty)=\Lambda_{\min}$. Since any periodic orbit embedded in the chaotic attractor has a positive Liapunov exponent, $\Lambda_{\min}$ cannot be negative for hyperbolic attractors. Therefore $0\leqq\Lambda_{\min}\leqq\Lambda_\infty(q)$ and $\Phi_\infty(q)\leqq\Phi_\infty(q')$ if $q<q'$. Since $\Phi_\infty(1)=0$, $\Phi_\infty(q)=\Lambda_{\max}q$ for $q\to-\infty$, $\Phi_\infty(q)=\Lambda_{\min}q$ for $q\to+\infty$, it thus turns out that $\Phi_\infty(q)$ behaves like Fig. 6, where $\Phi_\infty(q)$ lies between the two broken lines.

In the case of the SOM map, $\Phi_\infty(q)=-\ln|\nu(q)|$ is determined by the eigenvalue equation (4·4). We first determine $\Lambda_{\min}$ and $\Lambda_{\max}$. If we put $\nu=\hat{\nu}b^{q/(2m+1)}$, then (4·4) becomes

$$\hat{\nu}^{2m+1}-\sum_{i=m}^{2m}a_m{}^{q(2m-i)}b^{qi/(2m+1)}\,\hat{\nu}^i-\sum_{i=1}^{m-1}\{a_mb^{1/(2m+1)}\}^{qi}\,\hat{\nu}^i-1=0\,. \tag{B·1}$$

Since $a_m<1$, $b<1$, taking the limit $q\to+\infty$, we have

$$\hat{\nu}^{2m+1}-1=0\,. \tag{B·2}$$

This has the largest real solution $\tilde{\nu}=1$ so that we have

$$\nu(q)=b^{q/(2m+1)} \quad \text{for } q\to+\infty\,, \tag{B·3a}$$

$$\Lambda_{\min}=\Lambda_\infty(+\infty)=-\ln b/(2m+1)\,. \tag{B·3b}$$

It should be noted that $\Lambda_{\min}$ is the Liapunov exponent of a periodic orbit with period $(2m+1)$ which consists of orbit segments $\{x_t\}_{t=0}^{2m}$ such that $x_0\in I_1$, $x_1\in I_2$, $\cdots$, $x_{2m}\in I_{2m+1}$.

If we put $\nu=\tilde{\nu}b^q$, then (4·4) takes the form

$$\tilde{\nu}^{2m+1}-\tilde{\nu}^{2m}-\sum_{i=m}^{2m-1}(a_m/b)^{q(2m-i)}\tilde{\nu}^i-\sum_{i=0}^{m-1}(a_m/b)^{qi}b^{-2q(m-i)}\tilde{\nu}^i=0\,. \tag{B·4}$$

Since $b<a_m<1$, we have $(a_m/b)^q\to 0$, $b^{-q}\to 0$ as $q\to-\infty$ so that, taking the limit $q\to-\infty$, we have

$$\tilde{\nu}^{2m+1}-\tilde{\nu}^{2m}=0\,, \tag{B·5}$$

which leads to the largest real solution $\tilde{\nu}=1$. Hence we have

$$\nu(q)=b^q \quad \text{for } q\to-\infty\,, \tag{B·6a}$$

$$\Lambda_{\max}=\Lambda_\infty(-\infty)=-\ln b\,. \tag{B·6b}$$

$\Lambda_{\max}$ is the Liapunov exponent of the fixed point at $x=5/6$.

Now we take the limit $m\to\infty$. To get $\nu(q)$, it is convenient to carry out the summations in (4·4). Then we have

$$\nu^{2m+1}(\nu a_m{}^q-1)(\nu-a_m{}^q-b^q)-\nu^{m+1}a_m{}^{qm}(1-a_m{}^{2q})b^q+(\nu-a_m{}^q)b^q=0\,, \tag{B·7}$$

provided that $\nu\neq a_m{}^q$, $a_m{}^{-q}$.

[1] For $q>1$, it is clear from Fig. 6 that $\Lambda_{\min}(q-1)<\Phi_\infty(q)<\Lambda_{\min}q$. Inserting (B·3b) into the inequalities, we obtain

$$b^{(q-1)/(2m+1)}\geqq\nu(q)=\exp[-\Phi_\infty(q)]\geqq b^{q/(2m+1)}\,. \tag{B·8}$$

Hence, taking the limit $m\to\infty$, we have

$$\nu(q)=1\,. \tag{B·9}$$

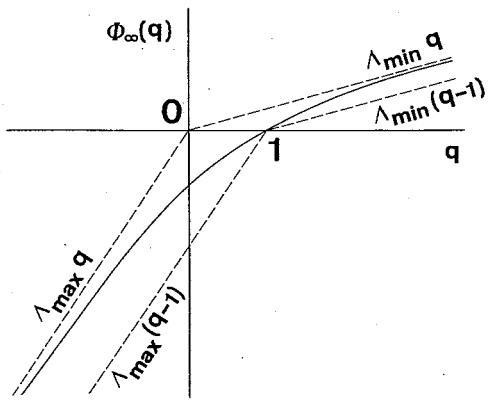


Fig. 6. Two broken lines between which $\Phi_\infty(q)$ lies.

[2] For $q<1$, we rewrite (B·7) as

$$\begin{aligned}&(\nu a_m{}^q-1)(\nu-a_m{}^q-b^q)\\&\quad-(a_m{}^q/\nu)^m(1-a_m{}^{2q})b^q\\&\quad+\nu^{-(2m+1)}(\nu-a_m{}^q)b^q=0\,,\end{aligned} \tag{B·10}$$

and assume that $\nu>1$. Since $\Phi_\infty(q)<\Lambda_{\max}q=-q\ln b$, $b<a_m<1$, we have $\nu(q)>b^q>a_m{}^q$ for $q<0$ and $\nu(q)>1\geqq a_m{}^q$ for $0\leqq q<1$. Therefore, in the limit $m\to\infty$, the second and third terms in (B·10) vanish so that we get

$$\nu(q)=a_c{}^q+b^q\,, \tag{B·11}$$

because $\nu=a_m{}^{-q}$ and $a_\infty=a_c=0.6$. Note that the solution (B·11) is valid if and only if the assumption $\nu>1$ is satisfied. However, the equation $a_c{}^q+b^q=1$ has the real solution $q=q_\delta\simeq 0.72716$, and $\nu(q\geqq q_\delta)\leqq 1$ violates the assumption. Thus, $\nu(q)\leqq 1$ for $q>q_\delta$. On the other hand, $\Phi_\infty(q<1)\leqq\Phi_\infty(1)=0$ so that $\nu(q<1)\geqq 1$. Therefore, we have $\nu(q)=1$ for $q_\delta\leqq q<1$.

From [1] and [2], the largest real solution $\nu(q)$ of (4·4) in the limit $m\to\infty$ turns out to be given by (4·5).

## Appendix C

*—— Relation Between K(q) and $\Phi_\infty(q)$ for a Piecewise Linear Markov map ——*

The generalized entropies $K(q)$ will be shown to be related to $\Phi_\infty(q)$ by $K(q)=\Phi_\infty(q)/(q-1)$ for a piecewise linear Markov map.

Introduce a sequence of $n$ subintervals $\{I_{i_1}, I_{i_2}, \cdots, I_{i_n}\}$ on the Markov partition $\{I_i\}_{i=1}^{M}$ such that

$$T_{i_n i_{n-1}} T_{i_{n-1} i_{n-2}} \cdots T_{i_2 i_1}=1\,, \tag{C·1}$$

where $T_{ij}$ is defined by (A·2). Then there exists an orbit $\{x_1, x_2, \cdots, x_n\}$ with $x_m\in I_{i_m}$. Consider a subinterval of $I_{i_1}$ in which the initial points $x_1$ of such orbits lie, i.e., a subinterval $I(i_1, i_2, \cdots, i_n)$ such that

$$\begin{aligned} &I(i_m, i_{m+1}, \cdots, i_n)\subset I_{i_m}\,,\\ &f(I(i_m, i_{m+1}, \cdots, i_n))=I(i_{m+1}, \cdots, i_n)\,,\\ &I(i_n)=I_{i_n} \end{aligned} \tag{C·2}$$

for $m=1, 2, \cdots, n-1$.

Let $P(i_1, i_2, \cdots, i_n)$ be the natural invariant measure of the subinterval $I(i_1, i_2, \cdots, i_n)$. Then the generalized entropies of the Markov map are given by

$$(q-1)K(q)=-\lim_{n\to\infty}(1/n)\ln\sum_{i_1,\cdots,i_n}{}' P^q(i_1, \cdots, i_n)\,, \tag{C·3}$$

where the sum $\sum'$ is taken over all possible sequences of $n$ subintervals $\{I_{i_1}, \cdots, I_{i_n}\}$ which satisfy (C·1).

Let $L(i_1, i_2, \cdots, i_n)$ be the length of the subinterval $I(i_1, i_2, \cdots, i_n)$. Then

$$\begin{aligned} L(i_1, i_2, \cdots, i_n)&=L(i_2, \cdots, i_n)/|f'_{i_1}|\\ &=L(i_n)/|f'_{i_1}f'_{i_2}\cdots f'_{i_{n-1}}|\,, \end{aligned} \tag{C·4}$$

where $f_i'$ denotes the value of the slope $f'(x)$ in $I_i$. Since $I(i_1, i_2, \cdots, i_n)\subset I_{i_1}$ and the invariant density $\rho(x)$ is uniform within $I_{i_1}$ with a value $\rho(i_1)$, we have

$$\begin{aligned} P(i_1, i_2, \cdots, i_n)&=\rho(i_1)L(i_1, i_2, \cdots, i_n)\\ &=\rho(i_1)L(i_n)/|f'_{i_1}f'_{i_2}\cdots f'_{i_{n-1}}|\,. \end{aligned} \tag{C·5}$$

Therefore, we have

$$\sum{}' P^q(i_1, i_2, \cdots, i_{n+1})$$
$$= \sum{}' \rho^q(i_1) |f'_{i_1} f'_{i_2} \cdots f'_{i_n}|^{-q} L^q(i_{n+1})$$
$$= [L^q(1), L^q(2), \cdots, L^q(M)] H_q{}^n \begin{bmatrix} \rho^q(1) \\ \rho^q(2) \\ \vdots \\ \rho^q(M) \end{bmatrix}, \qquad (C\cdot6)$$

where $H_q$ is the $M \times M$ matrix (A·6).

On the other hand, let us consider an orbit $\{x_1, \cdots, x_n\}$ with $x_m \in I_{i_m}$. Then the partition function (2·5) can be written as

$$Z_n(q) = \sum_{i_1, \cdots, i_n}{}' P(i_1, \cdots, i_n) |f'_{i_1} \cdots f'_{i_n}|^{-(q-1)}. \qquad (C\cdot7)$$

Therefore, using (C·5), we have

$$Z_n(q) = \sum{}' \rho(i_1) L(i_n) |f'_{i_1} \cdots f'_{i_n}|^{-q}$$
$$= [L(1), \cdots, L(M)] H_q{}^n \begin{bmatrix} \rho(1) \\ \vdots \\ \rho(M) \end{bmatrix}. \qquad (C\cdot8)$$

Similar to (3·6), (C·8) and (C·6) lead to

$$\lim_{n\to\infty} (1/n) \ln Z_n(q) = \ln |\nu(q)|,$$
$$\lim_{n\to\infty} (1/n) \ln \sum{}' P^q(i_1, \cdots, i_n) = \ln |\nu(q)|,$$

which are combined to give $(q-1)K(q) = \Phi_\infty(q)$.

## References


1) P. Bergé, Y. Pomeau and C. Vidal, *Order within Chaos* (Wiley, New York, 1984).
H. G. Schuster, *Deterministic Chaos* (VCH, Weinheim, 1988).
2) R. Bowen, *Equilibrium States and the Ergodic Theory of Anosov Diffeomorphisms,* Lect. Notes in Math. **470** (Springer, New York, 1975).
O. Lanford, *Entropy and Equilibrium States in Classical and Statistical Mechanics,* in: *Statistical Mechanics and Mathematical Problems,* ed. A. Lenard, Lect. Notes in Phys. **20** (Springer, New York, 1976).
D. Ruelle, *Thermodynamic Formalism* (Addison-Wesley, 1978).
3) J. Guckenheimer and P. Holmes, *Nonlinear Oscillations, Dynamical Systems and Bifurcations of Vector Fields* (Springer-Verlag, 1983).
4) T. C. Halsey, M. H. Jensen, L. P. Kadanoff, I. Procaccia and B. I. Shraiman, Phys. Rev. **A33** (1986), 1141.
M. H. Jensen, L. P. Kadanoff, A. Libchaber, I. Procaccia and J. Stavans, Phys. Rev. Lett. **55** (1985), 2798.
5) M. Sano, S. Sato and Y. Sawada, Prog. Theor. Phys. **76** (1986), 945.
6) J. -P. Eckmann and I. Procaccia, Phys. Rev. **A34** (1986), 659.
H. Fujisaka and M. Inoue, Prog. Theor. Phys. **77** (1987), 1334.
T. Bohr and D. Rand, Physica **25D** (1987), 387.
G. Paladin and A. Vulpiani, Phys. Rep. **156** (1987), 147.
7) T. Morita, H. Hata, H. Mori, T. Horita and K. Tomita, Prog. Theor. Phys. **78** (1987), 511; **79** (1988), 296.

8) H. Hata, T. Horita, H. Mori, T. Morita and K. Tomita, Prog. Theor. Phys. **80** (1988), 809.
T. Horita, H. Hata, H. Mori, T. Morita, K. Tomita, S. Kuroki and H. Okamoto, Prog. Theor. Phys. **80** (1988), 793.
K. Tomita, H. Hata, T. Horita, H. Mori and T. Morita, Prog. Theor. Phys. **80** (1988), 953.
9) T. Horita, H. Hata, H. Mori, T. Morita and K. Tomita, Prog. Theor. Phys. **81** (1989), 1.
10) Y. Pomeau and P. Manneville, Commun. Math. Phys. **74** (1980), 189.
11) J. E. Hirsch, B. A. Huberman and D. J. Scalapino, Phys. Rev. **A25** (1982), 519.
12) H. Mori, H. Okamoto, B. C. So and S. Kuroki, Prog. Theor. Phys. **76** (1986), 784.
13) N. Mori, S. Kuroki and H. Mori, Prog. Theor. Phys. **79** (1988), 1260.
14) K. Shobu, T. Ose and H. Mori, Prog. Theor. Phys. **71** (1984), 458.
15) H. Fujisaka and M. Inoue, Prog. Theor. Phys. **78** (1987), 268.
16) H. Fujisaka, Prog. Theor. Phys. **70** (1983), 1264; **71** (1984), 513.
17) R. S. Ellis, *Entropy, Large Deviations, and Statistical Mechanics* (Springer-Verlag, New York, 1985).
18) M. Dubois, M. A. Rubio and P. Bergé, Phys. Rev. Lett. **51** (1983), 1446.
19) H. Okamoto, H. Mori and S. Kuroki, Prog. Theor. Phys. **79** (1988), 581.
20) P. Szépfalusy, T. Tél, A. Csordás and Z. Kovács, Phys. Rev. **A36** (1987), 3525.